Results in Engineering 20 (2023) 101436

Contents lists available at ScienceDirect

Results in Engineering

journal homepage: www.sciencedirect.com/journal/results-in-engineering

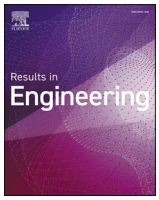

Electrochemical generation of ozone for application in environmental remediation

Leticia Mirella da Silva [a], Ismael F Mena [b], Miguel A. Montiel [b], Cristina Saez [b], Artur J. Motheo [a], Manuel A. Rodrigo [b,*]

[a] Instituto de Química de Sao Carlos, University of São Paulo São Carlos, Brazil
[b] Department of Chemical Engineering. Faculty of Chemical Sciences and Technologies. University of Castilla La Mancha, Campus Universitario s/n, 13071, Ciudad Real, Spain

ARTICLE INFO

Keywords:
Ozone
Continuous production
3-D printing
Mechanical design
Methomyl

ABSTRACT

This work focuses on the production, in continuous mode, of ozone using a new electrochemical cell, specially designed and manufactured with 3-D printing to produce in a very efficient way high concentrations of this powerful oxidant. The gaseous ozone produced is tested in the degradation of a synthetic waste containing methomyl. The new cell has been characterized in terms of flow distribution, mass transfer, and production of ozone, being able to reach efficiencies as high as 9.5 g/kWh, which may be even competitive with those produced with the corona discharge technology. The prototype manufactured with an electrode area of 1.5 cm^2 can produce a stream containing 30 mg/h of O_3. This stream can be used to degrade methomyl. However, the direct bubbling was not found to be very efficient and activation of ozone with the simultaneous irradiation of UV light or the dosing of hydrogen peroxide was needed to improve performance, showing important synergism. The efficient removal of methomyl from wastewater opens the window for the development of alternative technologies to direct anodic oxidation based on the production and dosing of gaseous oxidants such as ozone. The operation of these new technologies does not depend on the salts contained in wastewater and prevents the deterioration in the quality of the waste because it does not leave any residue after application in the treated waste.

1. Introduction

Gaseous oxidants produced electrochemically may have outstanding properties for their use in environmental applications over traditional electrochemical treatments [1–3]. They can be produced in situ and dosed directly to the polluted site, where they can reach more easily quiet zones in soils, because of the easier transport of gases through tortuous paths, or be more effective in liquids, as their dosing also attains better mixing conditions.

$$O_3 + 2H^+ + 2\ e^- \rightarrow O_2 + H_2O \quad (1)$$

Although chlorine dioxide is emerging as a very promising alternative [4], nowadays ozone is, perhaps, the most interesting gaseous oxidant that can be produced electrochemically [5]. It is a powerful oxidant with a wide range of applications in environmental remediation that has a primary advantage: its reduction product is oxygen and, hence, it lacks hazardousness (Equation (1)) [6–8].

$$3H_2O \rightarrow O_3 + 6H^+ + 6\ e^- \quad (2)$$

Although there are other more extended methods for its preparation, electrochemical technology has arisen as a good alternative in the last years [5] to the widely evaluated and applied corona discharge [9]. Thus, ozone is produced electrochemically by the oxidation of water throughout Equation (2), although at acidic conditions it may also come from the oxidation of oxygen (Equation (3)).

$$H_2O + O_2 \rightarrow O_3 + 2H^+ + 2\ e^- \quad (3)$$

$$2H_2O \rightarrow O_2 + 4H^+ + 4\ e^- \quad (4)$$

Both reactions compete with the formation of oxygen (Equation (4)) making necessary the application of large overpotentials to promote the production of ozone. Thus, the standard reduction potential required for Reaction 4 is E∘ = +1.23 V, while to produce ozone from water it raises

* Corresponding author.
E-mail address: manuel.rodrigo@uclm.es (M.A. Rodrigo).

https://doi.org/10.1016/j.rineng.2023.101436
Received 18 July 2023; Received in revised form 14 September 2023; Accepted 18 September 2023
Available online 22 September 2023

up to E∘ = +1.51 V [10].

Furthermore, it is possible to obtain higher ozone productions operating at higher pressures. Rodríguez-Peña et al. (2022) [11] demonstrated that the CabECO® cell (2.0 A) at 2 Bar gauge pressure reached the mark of 140 mg of ozone in discontinuous mode for 8 h. The same effect of increasing pressure on hydrogen peroxide generation is reported by Scialdone et al. (2015) [12] and Pérez et al. (2017) [13]. They obtained higher concentrations of H_2O_2 with the application of moderate (1–11 bar) [12] and high (30 bar) pressures [13]. However, with increasing pressure to produce more ozone, the amount of dissolved oxygen and the solubilization of the oxidant produced increases and the degradation pathways of organics become directly controlled by molecular ozone, decreasing the action of radical species [11].

There are two keys to reach an efficient electrochemical production: the selection of an efficient electrode and, the choice of an efficient electrochemical cell. In this context, diamond electrodes and PEM electrolyzers have been proposed as the most suitable alternative [5,11,14–17]. Electrodes consisting of diamond coatings have a large electrochemical window and promote the formation of hydroxyl radicals that cannot interact with the surface of the electrode, being available for reactions in the electrolyte in their extremely short lifetime [18]. One of the reactions that it is promoted is the formation of ozone [19]. On the other hand, in PEM electrolyzers, the electrolyte is not only the solution that it is flowing through the electrochemical cell but, more importantly, a proton exchange membrane that interacts directly (as membrane electrode assembly or MEA) with both electrodes allowing to balance the electric circuit of the cell with the protons that flow into the ionic circuit [20]. This fact shows two great advantages. The first is that cell voltage of the cell does not depend on the aqueous solution flow and ozone can be produced even with distilled water. The second, and more important, is that using a PEM electrolyzer prevents, or at least minimizes, the scavenging effect of salts contained in the liquid flowing within the cell. Production of other oxidants on the surface of the anode, such as peroxosulfate [21,22], peroxophosphates [23], peroxocarbonates [24], chlorine [25], etc., or hydrogen peroxide on the surface of the cathode [26,27], which results in a loss of efficiency of the electrochemical production of ozone, because these oxidants interact negatively with ozone promoting the formation of other non-stable oxidants such as sulfate, phosphate, chloride, carbonate, or hydroxyl radicals. However, although this effect is used in many environmental treatments because it enhances the degradation of organics (e.g. peroxone process) [6,19], it acts against good production [16].

Recently, 3-D printing has opened the possibility of developing tailored cells, a fact that has extreme importance in electrochemical technology, where efficiency and performance are very seriously affected by the mechanical design of the cell [28,29]. Thus, recently the design of cells with larger turbulence conditions and an easier evacuation of gases has demonstrated rather good enhancements in the performance of membrane-electrode assemblies, which is a very interesting point, which, in turn, is worth studying [14].

In this context, the goal pursued in this work is the development of a new concept of electrochemical cell in which ozone production is promoted. In addition, it is also aimed to test the ozone gaseous stream produced in the degradation of diluted solutions of methomyl, a carbamate insecticide used in this work as a model pollutant. 3-D design and printing will be used to manufacture a novel peripherical feeding electrochemical cell with enhanced performance, first used in this application.

2. Materials and methods

2.1. Chemicals

All solutions in this work were prepared with deionized water (Millipore Mili-Q system, resistivity 18.2 MΩ cm at 25 °C). Methomyl pestanal was purchased in Sigma Aldrich (Brazil) for calibration purposes. BrilhanteBR® (215 g/L of methomyl, Ourofino, Brazil) was employed as a commercial target compound for degradation in water solutions. For the determination of total oxidants potassium iodide 99,9% (Sigma-Aldrich) and sodium thiosulfate 0.5 N (Panreac) were used.

2.2. Experimental setup and procedure

The generation of ozone was carried out using a novelty proton-exchange membrane electrochemical cell (PEM) designed specifically for this work, which is inserted in a MEA with a Nafion® membrane and two lattice boron-doped diamonds (BDD) as electrodes. The cell was manufactured by 3-D printing, using a 3-D printer based on photopolymerization mechanism (ELEGOO MARS 2 PRO) using an acrylate polymeric resin (ELEGOO, Translucent ABS-Like Photopolymer Resin) was used to manufacture the electrochemical cell. After that, the pieces were cured in a Form Cure (Formalabs) at 70 °C for 1 h.

Fig. 1 shows a scheme of the electrochemical cell and the experimental set up. As can be seen, the electrochemical cell has been designed with two different compartments separated by the membrane. The compartments were designed to produce a centrifugal flow of the liquid phase and improve the gas relief in the cell. Two different tanks were used to accumulate the catholyte and anolyte, in this case, Milli-Q water (without the addition of any salt). The electrodes were connected to a power supply using a platinum thread. The gaseous ozone produced was extracted from the anodic tank and injected into the methomyl solution for the abatement of this compound.

2.3. Analytical techniques

The gaseous ozone produced was measured by the iodometric titration method. The gaseous oxidant was bubbled up in a KI solution (added in excess). After that, the sample was potentiometric titrated in acidic media with thiosulfate (0.001 N) using titration equipment (702 SM Titrino by Metrohm).

Methomyl concentration was analyzed by means of High-Performance Liquid Chromatography (HPLC) using an Agilent 1200 series coupled with a DAD detector at 223 nm and an analytical HPLC-DAD Zorbax Eclipse Plus C18 column (Agilent 1260 Infinity). The mobile phase was a mixture of formic acid (0.1%) and acetonitrile (80/20, v/v) at a flow rate of 0.3 cm^3/min^{-1}.

The energetic efficiency of ozone $\varepsilon O_3(mg/Wh)$ was calculated by Equation (5), where mO_3. represents the ozone production in mg/h and W is the applied power (W), estimated from the applied current i_{app} (A) and the observed average voltage T (V), according to Ref. [11].

$$\varepsilon O_3(mg\ /\ Wh) = \frac{mO_3}{W} \tag{5}$$

The efficiency of O_3 in terms of mg/A.min was estimated by Equation (6), where mO_3. represents the ozone production in mg/min.

$$O_3\ Efficiency\ (mg\ /\ A.min) = \frac{mO_3}{i_{app}} \tag{6}$$

The coulombic efficiency was estimated by the Equation (7), where mO_3 is the measured ozone production in mol/s and mO_3 *theoretical* is the theoretical prodution of ozone which, in turn, is related to the current applied (I), the electrons involved in the reaction (n) and the Faraday constant (F):

$$Coulombic\ Efficiency\ (\%) = \frac{mO_3}{mO_3\ theoretical} = \frac{mO_3}{\frac{I}{n \cdot F}} \tag{7}$$

3. Results and discussion

Continuous electrochemical production of ozone. Despite there are commercial electrochemical cells ready for ozone production with good

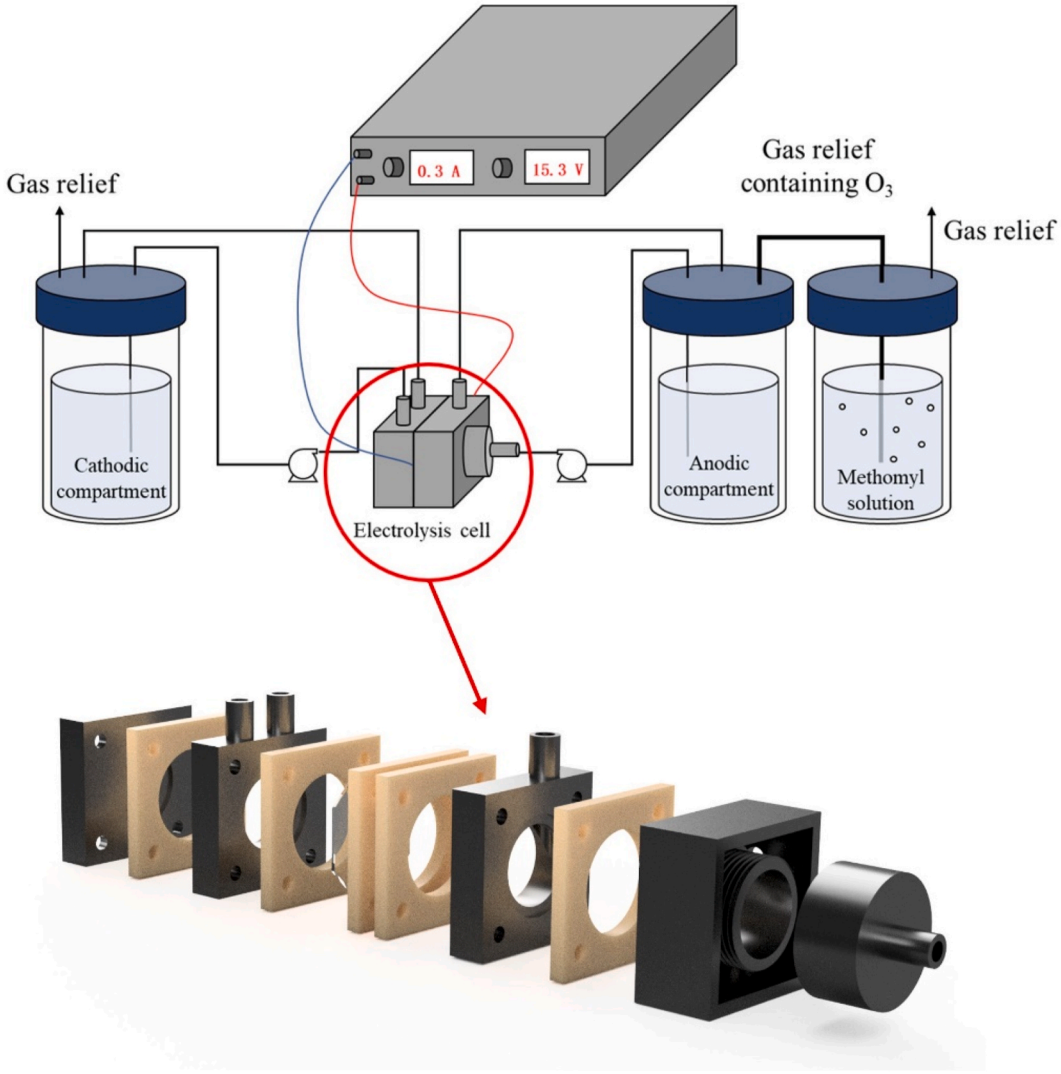

Fig. 1. Electrochemical cell design and a scheme of the experimental set up.

performance, for the specific application looked for in this work we considered the conceptualization, designing, and manufacturing with a 3D printer of a special cell, the so-called E3L ozone concept cell, for the efficient production of a gaseous stream of ozone, ready to be used in environmental applications. Target specifications required for the concept cell were two compartments to minimize the negative effects of scavengers on the production of ozone, a very effective flow distribution in the anodic chamber including a good separation of the gases formed, avoiding the accumulation of gases and the formation of dead volumes in the interelectrode volume, and operation at mild cell voltages. Because of the previous experience using different types of cells [5,10,11,14,15,17,30], PEM electrolyzers were fixed as a starting point. A special resin was used to prevent damage from ozone attack. The cell was sized for a flow rate of 14.4 L/h, electrode surface of 1.5 cm^2, and operation current intensity of 0.3 A, with a view to facilitate the staking to increase production capacity. During cell conceptualization, different prototypes were evaluated using CFD modelling and the best results from the viewpoint of an optimized flow distribution were the key to selecting the definitive concept prototype. In fact, centrifugal flow patterns were found to be of the greatest interest, and different models were simulated. Fig. 2 shows, with the concept of centrifugal flow outlet, the flow lines in one prototype with a central inlet and another with a peripherical inlet, which were found from the very beginning to be the more suitable approaches for this cell.

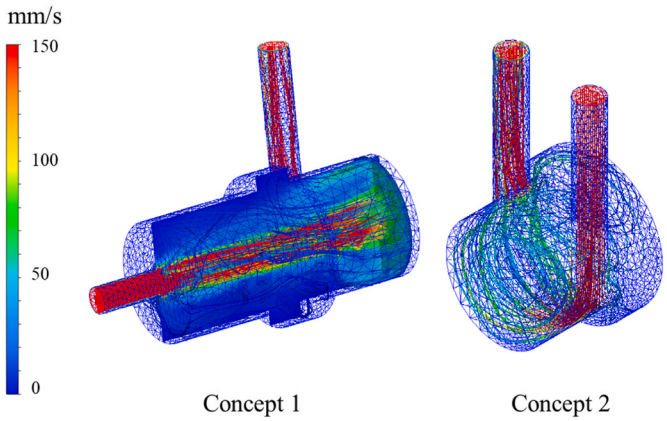

Fig. 2. CFD simulation of the designed concept for the electrochemical cell. Linear velocity vector of the flow is represented in mm/s.

The flow rate fed to the cell is of extreme importance to reach a good performance. These cells produced a gaseous outlet flow, but the liquid electrolyte is continuously recirculated between a storage tank and the cell, and it has the purpose of dragging gases produced and keeping the MEA wet while acting as a secondary electrolyte (in addition to the

membrane contained in the MEA). Considering that, the E3L ozone production concept cell was designed for an electrolyte flowrate recirculation capacity as low as 14.4 L/h. Figs. 2 and 3 show the flow velocity profiles calculated by CFD simulation and also include a graph indicating the percentage of the electrode surface area in which the flow velocity is below 20 mm/s. As seen, the central feeding allows a more suitable flow distribution, and for the nominal flow rate less than 2% of the surface has a surface flow velocity below 20 mm/s. This value increases six times when using the peripherical feeding. However, the direct impact of the flow against the MEA was considered as a weak point because it may affect the service lifetime of this assembly (see Fig. 4).

Fig. 5 shows the DTR curves of the two types of compartments previously described and the fitting parameters to a model that provides the Peclet and the average hydraulic retention time. A good fit was observed, with extremely low Peclet numbers (<0.3), indicating a large distribution in both electrochemical compartments. Moreover, mean residence times are in the range of 3–12 s, which is similar in both concepts. The Figure also includes the mass transfer coefficients calculated by the ferro-ferricyanide technique, which result in values extremely high as compared to those obtained by other electrochemical cells studied in the literature [31,32].

With these inputs, the cell integrated is used for the anodic compartment the central feeding, and for the cathodic the peripherical, trying to minimize the damages in the MEA produced by the impact of the two opposite flows and take advantage of the compartment where ozone is produced of the more efficient central feeding. Thus, the effect of current intensity, temperature, and ozone production were evaluated, these parameters are known to be the most important inputs according to previous studies.

The influence of current density is shown in Fig. 6, where it can be observed that although the higher productions are obtained at the highest current density tested of 200 mA/cm^2, the most efficient conditions involve the operation at 150 mA/cm^2, where the coulombic efficiency reach values as high as 50% and the energy efficiency almost reached 10 mg O_3/Wh, values that are over those reported in the literature [11,14], demonstrated in Table 1. Table 1 shows the comparison in terms of energy consumption (power) and energy efficiency when compared to other similar works. Under these conditions, the E3L cell was able to produce 30 mg/h with an electrode as tiny as 1.5 cm^{-2}.

Another similar work found, using an ozone generator with PEM membrane and lead dioxide nanowires [33], using a 3 × 3 cm^2 electrode, operating with a current density of 1.5 A cm^{-2} was able to achieve a constant potential differential of 3.45 V and current efficiency of only 20% during 30 days of operation. In this work, it was achieved almost 50% of coulombic efficiency using an electrode with working area of 1.5 cm^2 and applying 150 mA/cm^2 at 25 °C.

The influence of temperature is shown in Fig. 7, where three tests were carried out at the same current density of 150 mA/cm^2. Temperature has a slight positive effect with coulombic efficiencies that reached values as high as 50% and energy efficiencies over 8 mg O_3/Wh. The highest production of ozone is reached using the highest temperature due to an increase in temperature favoring the desorption of ozone from the water and, consequently, its extraction from the system in the gaseous phase.

Using electrochemically produced ozone for degradation of methomyl. To verify the suitability of using indirect electrolysis for environmental applications, the gaseous flow of ozone was bubbled into a solution containing methomyl. Trying to promote the action of ozone the combination with hydrogen peroxide and UV was also tested. As seen in Figs. 8 and 9, ozone is not very efficient itself for the degradation of methomyl or in the degradation of the other species contained in the commercial product. The same applies to hydrogen peroxide, which suggests the refractory character of methomyl and that chemical oxidation of the organic is not promoted. However, when combined with hydrogen peroxide in the same concentration of ozone or, especially with a UV light with a power of 1 W (which has an outstanding performance) it results in a very synergistic effect. Both activators promote the formation of radicals from ozone, and it may be explained by the improvement in the performance with radical oxidation mechanisms as previously demonstrated by Chang et al., 2015 [34]. They demonstrate that the combination of UV-C radiation with the produced ozone, induces the decomposition of O_3 to form hydroxyl ($OH^{\bullet}$) radical, enhancing the oxidizing ability of the solution. Also, the H_2O_2 can be decomposed to form $OH^{\bullet}$ radicals via ozonation. The mechanisms of UV-Ozone and H_2O_2-Ozone in an aqueous solution can be depicted below, extracted from Refs. [34,35]:

$$O_3 + H_2O \xrightarrow{h\nu} O_2 + H_2O_2$$

$$O_3 + H_2O \xrightarrow{h\nu} O_2 + 2OH^{\bullet}$$

The hydrogen peroxide decomposition by ozone:

$$H_2O_2 \leftrightarrow HO_2^- + H^+$$

$$HO_2^- + O_3 \rightarrow HO_2^{\bullet} + O_3^{\bullet -}$$

$$O_3^{\bullet -} + H^+ \rightarrow HO_3^{\bullet} \rightarrow OH^{\bullet} + O_2$$

All processes, bare ozone or ozone activated by UV or hydrogen peroxide, do not leave in the solution any waste after the application because ozone is transformed into oxygen and no other reagents need to be dosed. In addition, there is no need to add salts to the waste treated, like in direct anodic oxidation processes, in which salts are added to decrease cell voltage and promote the production of oxidants. In this

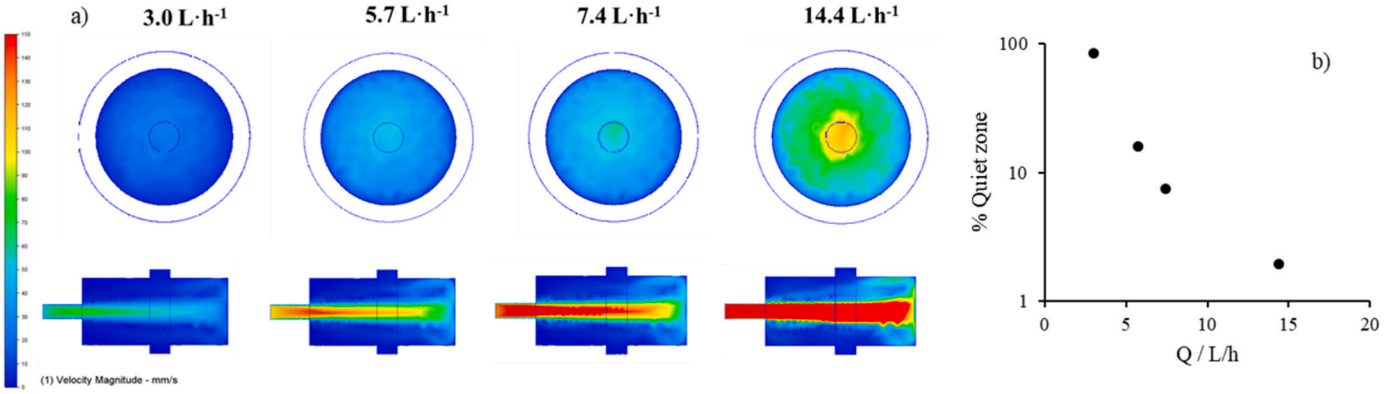

Fig. 3. a) CFD simulation of the designed concept 1 at different flows (3.0 L/h; 5.7 L/h; 7.4 L/h and 14.4 L/h) where the linear velocity vector is represented (mm/s) and b) percentage of dead zones (zones with a flow velocity lower than 20 mm/s) on the electrode surface.

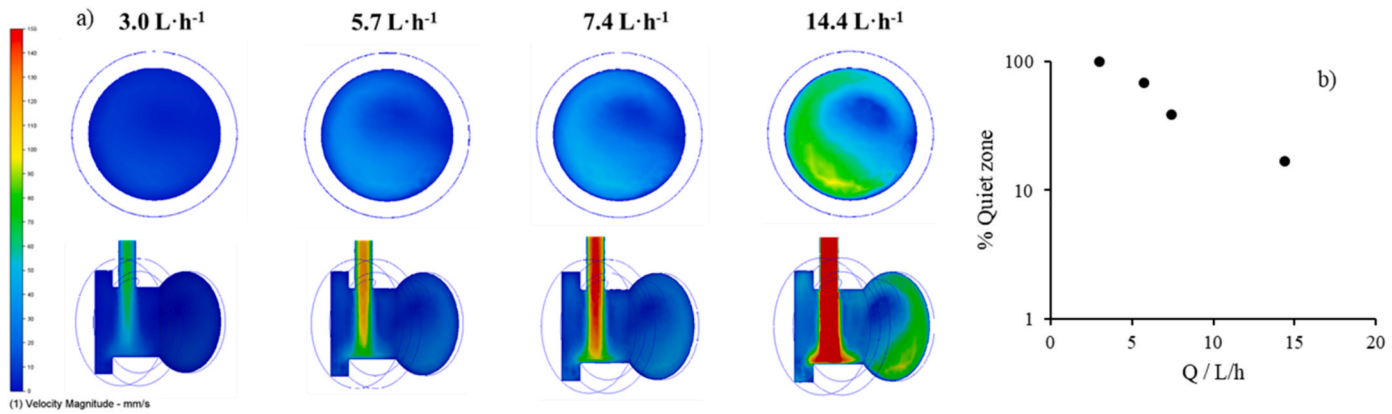

Fig. 4. a) CFD simulation of the designed concept 2 at different flows (3.0 L/h; 5.7 L/h; 7.4 L/h and 14.4 L/h) where the linear velocity vector is represented (mm/s) and b) percentage of dead zones (zones with a flow velocity lower than 20 mm/s) on the electrode surface.

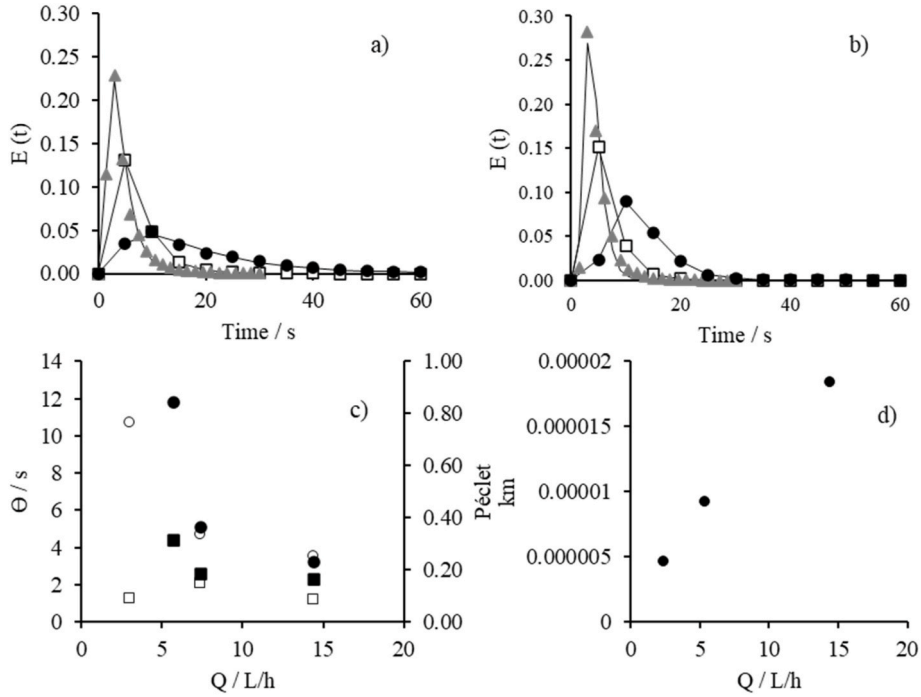

Fig. 5. DTR curves of a) designed concept 1 at different flows (circles: 5.7 L/h; squares: 7.4 L/h; triangles: 14.4 L/h) and b) designed concept 2 at different flows (circles: 3.0 L/h; squares: 7.4 L/h; triangles: 14.4 L/h). c) Mean residence time (circles) and Péclet number (squares) of designed concept 1 (black) and designed concept 2 (white) compartments. d) Mass transfer coefficients at different flowrates using the central feeding as an anodic compartment and the peripherical for the cathodic compartment.

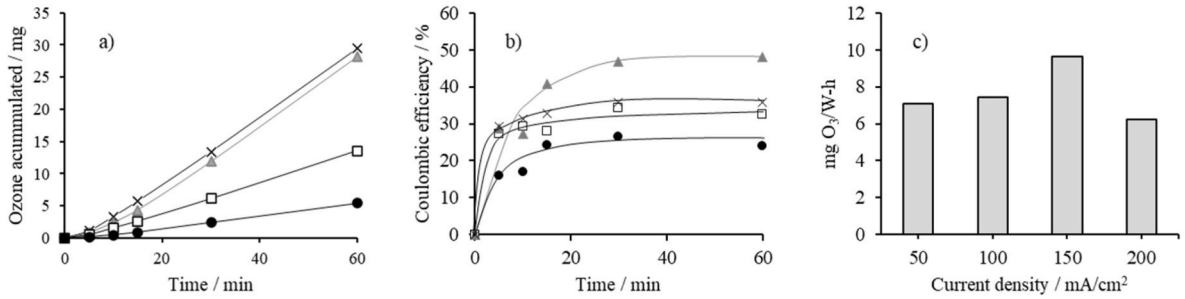

Fig. 6. Ozone accumulated (a), Coulombic efficiency (b), and energetic efficiency (c) at different current densities (circles: 50 mA/cm^2; squares: 100 mA/cm^2; triangles: 150 mA/cm^2; crosses: 200 mA/cm^2) using a temperature of 15 °C, O_2 flow of 20 mL/h, mQ water as a solution.

Table 1
Comparison of coulombic efficiency and power consumption of the new cell with literature.

Cell	j/mA/cm^2	Power/W	O_3 Efficiency/mg/(A·min)	Reference
CabECO	83.3	12	0.085	[12]
Condiapure	68.5	80	0.013	[12]
PEM cell	330	313.17	0.335	[8]
E3L	50	0.77	1.190	This work
E3L	100	1.83	1.162	This work
E3L	150	2.92	2.393	This work
E3L	200	4.74	1.783	This work

case, the gaseous ozone is produced in a system separated from the degradation tank where the gaseous ozone is being dosed to treat the methomyl solution. This means that the process is cleaner and, therefore, more sustainable for the environment, confirming the good prospects of the gaseous oxidants mediated electrochemical technology (GOMET) using ozone for the remediation of wastes and encouraging research in this topic.

4. Conclusions

From this work, the following conclusions can be drawn.

- Ozone can be produced efficiently by using PEM electrolyzer technology.
- A concept cell (so-called E3L ozone production concept cell) has been conceptualized, designed, and manufactured using 3-D printing for ozone gas production. This cell reaches outstanding performances and can produce (with an electrode surface area of 1.5 cm^2) close to 30 mg/h of ozone. This means a coulombic efficiency of around 50% and an energy efficiency of 9.5 mg O_3/Wh, among the highest ever reported.
- Ozone produced electrochemically can be used to degrade methomyl contained in synthetic wastes. However, this process has low efficiency and the ozone produced needs to be activated (transformed into radicals) by another oxidant, such as hydrogen peroxide or UV light, to obtain greater efficiency in methomyl removal. This demonstrates the feasibility and good prospects of gaseous oxidants mediated electrochemical technologies (GOMET) for wastewater remediation.

Credit author statement

Leticia M. da Silva: Investigation, Data curation, Formal analysis, Writing – original draft. Ismael Fernandez Mena: Investigation, Data curation, Formal analysis, Writing – original draft. Miguel A. Montiel:

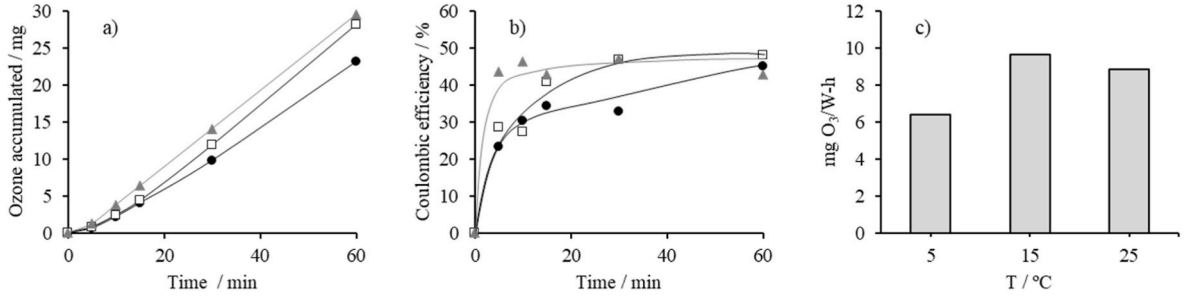

Fig. 7. Ozone accumulated (a), Coulombic efficiency (b), and energetic efficiency (c) at different temperatures (circles: 5 °C; squares: 15 °C; triangles: 25 °C) using a current intensity of 150 mA/cm^2, O_2 flow of 20 mL/h, mQ water as a solution.

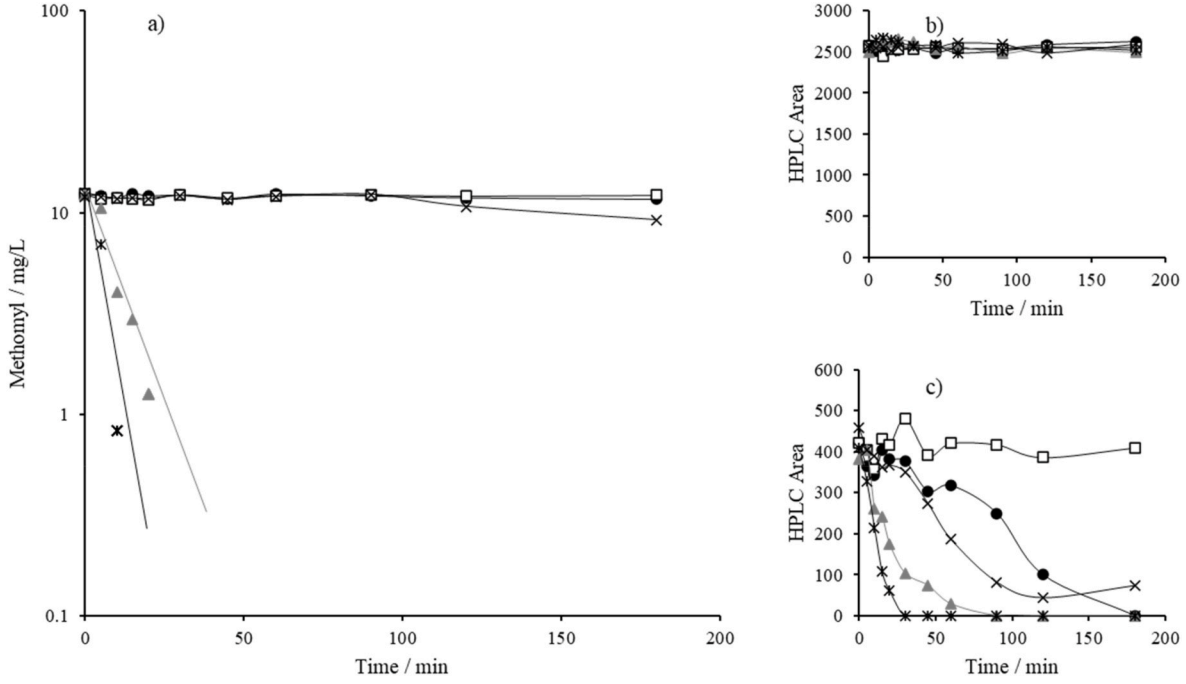

Fig. 8. a) Methomyl degradation, b) chromatograph peak detected at 4.3 min, and c) chromatograph peak detected at 7 min in the different treatments studied (circles: O_3; squares: H_2O_2; triangles: UV; crosses: O_3/H_2O_2; stars: O_3/UV).

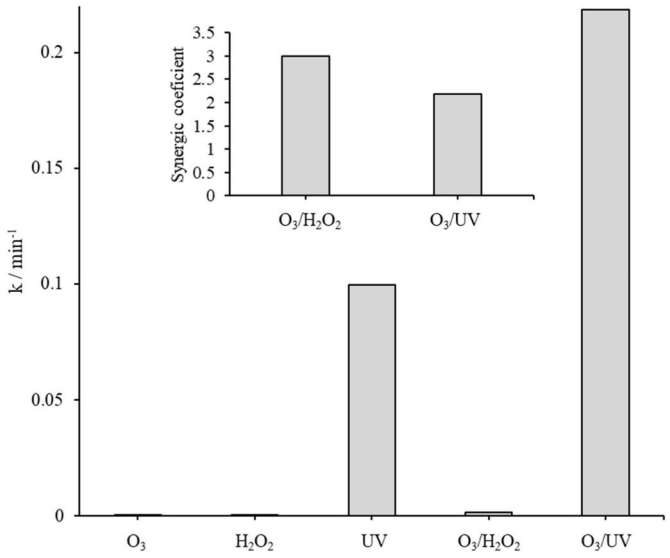

Fig. 9. Pseudo-first order kinetic constant degradation of the different technologies applied for the methomyl degradation. Insert: Synergic coefficient in O_3/UV and O_3/H_2O_2.

Writing – review & editing. Cristina Saez: Writing – review & editing. Artur J. Motheo: Writing – review & editing, Funding acquisition, Project administration, Supervision, Validation, Writing – review & editing. Manuel A. Rodrigo: Conceptualization, Funding acquisition, Project administration, Supervision, Validation, Writing – review & editing.

Declaration of competing interest

The authors declare that they have no known competing financial interests or personal relationships that could have appeared to influence the work reported in this paper.

Data availability

Data will be made available on request.

Acknowledgements

This work comprises the research projects PID2022-138401OB-I00 and PCI2021-121963 granted by MCIN/AEI/10.13039/501100011033/ and "European Union Next Generation EU/PRTR".

References

[1] S.V. Manjunath, B.R. Yakshith, M. Meghashree, Synergistic analysis for co-treatment of poultry wastewater and sewage in electro-chemical system: operational parameters, kinetics and energy estimation, Results in Eng. 19 (2023), 101275, https://doi.org/10.1016/j.rineng.2023.101275.

[2] O.J. Ajala, J.O. Tijani, R.B. Salau, A.S. Abdulkareem, O.S. Aremu, A review of emerging micro-pollutants in hospital wastewater: environmental fate and remediation options, Results in Eng. 16 (2022), https://doi.org/10.1016/j.rineng.2022.100671.

[3] P.O. Oladoye, T.O. Ajiboye, E.O. Omotola, O.J. Oyewola, Methylene blue dye: toxicity and potential elimination technology from wastewater, Results in Eng. 16 (2022), https://doi.org/10.1016/j.rineng.2022.100678.

[4] M.K. Sales Monteiro, M.M. Sales Monteiro, A.M. de Melo Henrique, J. Llanos, C. Saez, E.V. Dos Santos, M.A. Rodrigo, A review on the electrochemical production of chlorine dioxide from chlorates and hydrogen peroxide, Curr. Opin. Electrochem. 27 (2021), https://doi.org/10.1016/j.coelec.2020.100685.

[5] M. Rodríguez-Peña, J.A. Barrios Pérez, J. Llanos, C. Sáez, M.A. Rodrigo, C. E. Barrera-Díaz, New insights about the electrochemical production of ozone, Curr. Opin. Electrochem. 27 (2021), https://doi.org/10.1016/j.coelec.2021.100697.

[6] Y. Mao, D. Guo, W. Yao, X. Wang, H. Yang, Y.F. Xie, S. Komarneni, G. Yu, Y. Wang, Effects of conventional ozonation and electro-peroxone pretreatment of surface water on disinfection by-product formation during subsequent chlorination, Water Res. 130 (2018) 322–332, https://doi.org/10.1016/j.watres.2017.12.019.

[7] F. Bu, B. Gao, X. Shen, W. Wang, Q. Yue, The combination of coagulation and ozonation as a pre-treatment of ultrafiltration in water treatment, Chemosphere 231 (2019) 349–356, https://doi.org/10.1016/j.chemosphere.2019.05.154.

[8] A. John, A. Brookes, I. Carra, B. Jefferson, P. Jarvis, Microbubbles and their application to ozonation in water treatment: a critical review exploring their benefit and future application, Crit. Rev. Environ. Sci. Technol. 52 (2022) 1561–1603, https://doi.org/10.1080/10643389.2020.1860406.

[9] C.V. Rekhate, J.K. Srivastava, Recent advances in ozone-based advanced oxidation processes for treatment of wastewater- A review, Chemical Eng. J. Adv. 3 (2020), https://doi.org/10.1016/j.ceja.2020.100031.

[10] M. Rodríguez-Peña, J.A.B. Pérez, J. Llanos, C. Saez, C.E. Barrera-Díaz, M. A. Rodrigo, Understanding ozone generation in electrochemical cells at mild pHs, Electrochim. Acta 376 (2021), https://doi.org/10.1016/j.electacta.2021.138033.

[11] M. Rodríguez-Peña, J.A. Barrios Pérez, J. Lobato, C. Saez, C.E. Barrera-Díaz, M. A. Rodrigo, Influence of pressure and cell design on the production of ozone and organic degradation, Sep. Purif. Technol. 297 (2022), https://doi.org/10.1016/j.seppur.2022.121529.

[12] O. Scialdone, A. Galia, C. Gattuso, S. Sabatino, B. Schiavo, Effect of air pressure on the electro-generation of H2O2 and the abatement of organic pollutants in water by electro-Fenton process, Electrochim. Acta 182 (2015) 775–780, https://doi.org/10.1016/j.electacta.2015.09.109.

[13] J.F. Pérez, A. Galia, M.A. Rodrigo, J. Llanos, S. Sabatino, C. Sáez, B. Schiavo, O. Scialdone, Effect of pressure on the electrochemical generation of hydrogen peroxide in undivided cells on carbon felt electrodes, Electrochim. Acta 248 (2017) 169–177, https://doi.org/10.1016/j.electacta.2017.07.116.

[14] I.F. Mena, M.A. Montiel, C. Sáez, M.A. Rodrigo, Improving performance of proton-exchange membrane (PEM) electro-ozonizers using 3D printing, Chem. Eng. J. 464 (2023), https://doi.org/10.1016/j.cej.2023.142688.

[15] M. Rodríguez-Peña, J.A. Barrios Pérez, J. Llanos, C. Saez, C.E. Barrera-Díaz, M. A. Rodrigo, Is ozone production able to explain the good performance of CabECO® technology in wastewater treatment? Electrochim. Acta 396 (2021) https://doi.org/10.1016/j.electacta.2021.139262.

[16] M. Rodríguez-Peña, I.F. Mena, J.A.B. Pérez, C.E. Barrera-Díaz, M.A. Rodrigo, Does electro-peroxonation improve performance of electro-ozonation? J. Environ. Chem. Eng. 10 (2022) https://doi.org/10.1016/j.jece.2022.107578.

[17] M. Rodríguez-Peña, J.A. Barrios Pérez, J. Llanos, C. Saez, C.E. Barrera-Díaz, M. A. Rodrigo, Toward real applicability of electro-ozonizers: paying attention to the gas phase using actual commercial PEM electrolyzers technology, Chemosphere 289 (2022), https://doi.org/10.1016/j.chemosphere.2021.133141.

[18] Y. Honda, T.A. Ivandini, T. Watanabe, K. Murata, Y. Einaga, An electrolyte-free system for ozone generation using heavily boron-doped diamond electrodes, Diam. Relat. Mater. 40 (2013) 7–11, https://doi.org/10.1016/j.diamond.2013.09.001.

[19] G. Acosta-Santoyo, L.F. León-Fernández, E. Bustos, P. Cañizares, M.A. Rodrigo, J. Llanos, On the production of ozone, hydrogen peroxide and peroxone in pressurized undivided electrochemical cells, Electrochim. Acta 390 (2021), https://doi.org/10.1016/j.electacta.2021.138878.

[20] P.A. Christensen, T. Yonar, K. Zakaria, The electrochemical generation of ozone: a review, Ozone Sci. Eng. 35 (2013) 149–167, https://doi.org/10.1080/01919512.2013.761564.

[21] G. Divyapriya, P.V. Nidheesh, Electrochemically generated sulfate radicals by boron doped diamond and its environmental applications, Curr. Opin. Solid State Mater. Sci. 25 (2021), https://doi.org/10.1016/j.cossms.2021.100921.

[22] K.C.F. Araújo, K.N.O. Silva, M.K.S. Monteiro, D.R. da Silva, M.A. Quiroz, E.V. dos Santos, C.A. Martínez-Huitle, Towards use of persulfate electrogenerated at boron doped diamond electrodes as ex-situ oxidation approach: storage and service-life solution parameters, J. Electrochem. Soc. 169 (2022), 033506, https://doi.org/10.1149/1945-7111/ac59f8.

[23] A. Sánchez, J. Llanos, C. Sáez, P. Cañizares, M.A. Rodrigo, On the applications of peroxodiphosphate produced by BDD-electrolyses, Chem. Eng. J. 233 (2013) 8–13, https://doi.org/10.1016/j.cej.2013.08.022.

[24] K. Groenen Serrano, A critical review on the electrochemical production and use of peroxo-compounds, Curr. Opin. Electrochem. 27 (2021), https://doi.org/10.1016/j.coelec.2020.100679.

[25] G.O.S. Santos, K.I.B. Eguiluz, G.R. Salazar-Banda, C. Sáez, M.A. Rodrigo, Understanding the electrolytic generation of sulfate and chlorine oxidative species with different boron-doped diamond anodes, J. Electroanal. Chem. 857 (2020), https://doi.org/10.1016/j.jelechem.2019.113756.

[26] J.F. Pérez, J. Llanos, C. Sáez, C. López, P. Cañizares, M.A. Rodrigo, Electrochemical jet-cell for the in-situ generation of hydrogen peroxide, Electrochem. Commun. 71 (2016) 65–68, https://doi.org/10.1016/j.elecom.2016.08.007.

[27] S. Siahrostami, S.J. Villegas, A.H. Bagherzadeh Mostaghimi, S. Back, A.B. Farimani, H. Wang, K.A. Persson, J. Montoya, A review on challenges and successes in atomic-scale design of catalysts for electrochemical synthesis of hydrogen peroxide, ACS Catal. 10 (2020) 7495–7511, https://doi.org/10.1021/acscatal.0c01641.

[28] A. Ambrosi, M. Pumera, 3D-printing technologies for electrochemical applications, Chem. Soc. Rev. 45 (2016) 2740–2755, https://doi.org/10.1039/c5cs00714c.

[29] B. Regassa Hunde, A. Debebe Woldeyohannes, Future prospects of computer-aided design (CAD) – a review from the perspective of artificial intelligence (AI), extended reality, and 3D printing, Results in Eng. 14 (2022), https://doi.org/10.1016/j.rineng.2022.100478.

[30] M. Rodríguez-Peña, J.A. Barrios Pérez, J. Llanos, C. Saez, C.E. Barrera-Díaz, M. A. Rodrigo, Electrochemical generation of ozone using a PEM electrolyzer at acidic

pHs, Sep. Purif. Technol. 267 (2021), https://doi.org/10.1016/j.seppur.2021.118672.
[31] A.M. Polcaro, A. Vacca, M. Mascia, S. Palmas, R. Pompei, S. Laconi, Characterization of a stirred tank electrochemical cell for water disinfection processes, Electrochim. Acta 52 (2007) 2595–2602, https://doi.org/10.1016/j.electacta.2006.09.015.
[32] C.N. Brito, M.B. Ferreira, E.C.M. de Moura Santos, J.J.L. Léon, S.O. Ganiyu, C. A. Martínez-Huitle, Electrochemical degradation of Azo-dye Acid Violet 7 using BDD anode: effect of flow reactor configuration on cell hydrodynamics and dye removal efficiency, J. Appl. Electrochem. 48 (2018) 1321–1330, https://doi.org/10.1007/s10800-018-1257-4.
[33] S. Chen, F. Jiang, X. Xie, Y. Zhou, X. Hu, Synthesis and application of lead dioxide nanowires for a PEM ozone generator, Electrochim. Acta 192 (2016) 357–362, https://doi.org/10.1016/j.electacta.2016.01.202.
[34] C.C. Chang, C. Trinh, C.Y. Chiu, C.Y. Chang, S.W. Chiang, D.R. Ji, J.Y. Tseng, C. F. Chang, Y.H. Chen, UV-C irradiation enhanced ozonation for the treatment of hazardous insecticide methomyl, J. Taiwan Inst. Chem. Eng. 49 (2015) 100–104, https://doi.org/10.1016/j.jtice.2014.11.001.
[35] G.R. Peyton, W.H. Glaze, Destruction of Pollutants in Water with Ozone in Combination with Ultraviolet Radiation. 3. Photolysis of Aqueous Ozone, 1988. https://pubs.acs.org/sharingguidelines.